NACA RM H57D18b

RESEARCH MEMORANDUM

FLIGHT MEASUREMENTS OF AIRPLANE STRUCTURAL TEMPERATURES AT SUPERSONIC SPEEDS

By Richard D. Banner

High-Speed Flight Station
Edwards, Calif.

NATIONAL ADVISORY COMMITTEE
FOR AERONAUTICS

WASHINGTON

June 7, 1957
Declassified July 22, 1959

NATIONAL ADVISORY COMMITTEE FOR AERONAUTICS

RESEARCH MEMORANDUM

FLIGHT MEASUREMENTS OF AIRPLANE STRUCTURAL TEMPERATURES AT SUPERSONIC SPEEDS

By Richard D. Banner

SUMMARY

Skin and structural temperatures have been obtained on the X-1B and X-1E research airplanes under transient aerodynamic heating conditions at speeds up to Mach numbers near 2.0. Extensive temperature measurements were obtained throughout the X-1B airplane, and temperature distributions are shown on the nose cone, the wing, and the vertical tail. Temperatures for the X-1E wing leading edge and internal wing structure were compared with similar data for the X-1B.

No critical skin and structural temperatures were obtained on the two airplanes over the range of these tests.

Simplified calculations of the skin temperatures in the laminar-flow regions of the nose cone and the leading edges agreed favorably with the general trends in the measured data. The flat-plate skin-temperature calculations in the turbulent-flow regions agreed favorably with the measured data on the nose cone and at the midsemispan station of the wing but overestimated the vertical-tail skin temperatures and also the upper wing skin temperature near the wing tip. The relatively low values of the upper skin temperatures that were measured at the wing tip were believed to be caused by separated-flow effects in this region.

INTRODUCTION

In the design of supersonic aircraft, aerodynamic heating is becoming increasingly important. Analytical studies and controlled testing represent the basic methods utilized in the design of complex structures to withstand the effects of aerodynamic heating.

Concurrent with the basic research studies, the National Advisory Committee for Aeronautics is conducting a program at the NACA High-Speed Flight Station at Edwards, Calif., to investigate the skin and structural temperatures actually experienced by airplanes during flight at supersonic speeds. The purpose of this paper is to summarize the results of

this program to the present time. The results of simplified calculations of the skin temperatures are compared with the measured data in the regions of the fuselage nose cone and the wing and vertical-tail skins and leading edges.

SYMBOLS

$b/2$	wing semispan
c	chord length
h_{av}	average heat-transfer coefficient, Btu/sq ft-hr-$^{\circ}$F
h_p	pressure altitude, ft
M	Mach number
P	local surface pressure, lb/sq ft
P_∞	free-stream static pressure, lb/sq ft
q_∞	free-stream dynamic pressure, lb/sq ft
r	recovery factor
T	skin temperature, $^{\circ}$F
T_{aw}	adiabatic wall temperature, $^{\circ}$F
T_T	free-stream stagnation temperature, $T_\infty(1 + 0.2M^2)$, $^{\circ}$F
T_∞	free-stream ambient air temperature, $^{\circ}$F
t	time, sec
α	angle of attack, deg
τ	thickness, in.

TESTS

Data have recently been obtained on the X-1E airplane at Mach numbers up to 2.10 and on the X-1B at Mach numbers up to 1.94. (See fig. 1.)

These speeds do not necessarily represent the maximum speed capabilities of the airplanes. Both airplanes are constructed primarily of aluminum. Temperature measurements were made at approximately 60 locations on the X-1E, and approximately 300 temperatures were measured on the X-1B.

Figure 2 shows the flight conditions for both airplanes under which the temperatures were obtained. The Mach number, pressure altitude, ambient air temperature, and angle of attack are shown as time histories. As can be seen, the two flights are generally similar.

Transient heating conditions were experienced by both airplanes during the flights. The maximum heating rate was experienced on the thinner skinned X-1B and was on the order of 3° per second. This heating rate is relatively low in comparison with the rates being obtained on missiles and rocket models and in controlled wind-tunnel tests; however, it is believed to be representative of the heating rates which are being experienced or which will be experienced in the near future by fighter and interceptor aircraft.

CALCULATIONS

For laminar flow in the stagnation regions, approximate heat-transfer coefficients were calculated from expressions relating the Nusselt number and the Reynolds number given by Stine and Wanlass. (See ref. 1.) In the regions of flat-plate turbulent flow, approximate heat-transfer coefficients were calculated by using Colburn's expression. These calculations were greatly simplified by the use of free-stream conditions. This procedure was considered justified in that only the overall effects were desired. A detailed theoretical analysis is not considered to be within the scope of this report.

The results of the calculations just described indicated relatively small variations in the heat-transfer coefficients with time; therefore, average values were determined and used in calculating the skin temperatures.

Newton's law of heat flow to the skin, which considers the heat capacity of the material and neglects the effects of conduction, was assumed.

RESULTS AND DISCUSSION

The X-1B installation provides a rather detailed case history of the temperatures that exist throughout an actual airplane; and, in view of this fact, more attention is given to the X-1B data in the present paper.

The X-1E data are used to point out any differences that exist in the measured temperatures due to either the configuration or the construction or both.

Some of the maximum temperatures that were measured on the X-1B and an indication of the higher temperature areas on the airplane are shown in figure 3. The nose of the airplane and the leading edges of the wing and tail surfaces are shaded in figure 3 to indicate the higher temperature areas. The approximate thermocouple locations are indicated by the dark points. The maximum stagnation temperature for the flight was 220° F.

A maximum skin temperature of 185° F was measured at the forward point of the nose cone. On the wing leading edge the maximum temperature was 168° F. A maximum temperature on this order was also measured on the leading edge of the vertical tail. The maximum temperatures in other general areas are also shown. Some of the temperatures shown at these locations are appreciably affected by internal heat sources and heat sinks; for instance, the fuselage skin temperatures adjacent to the liquid oxygen tank are relatively low (13° F); whereas, just ahead of that area on the fuselage skin a maximum of 122° F was measured. Other areas of interest are the windshield and canopy and the rearward part of the fuselage in the region of the rocket engine.

It should be pointed out that the maximum temperatures shown in figure 3 did not all occur at the same time. In areas where internal conduction is negligible, skin thickness, boundary-layer temperature, and the heat-transfer coefficient are the primary factors affecting the skin temperature rise.

Figure 3 gives an overall picture of the measured temperatures. In subsequent figures, the temperature distributions in the areas of the nose cone, the wing skins, the leading edges and the vertical tail are considered in greater detail; and comparisons are made with calculated results. Attention is given only to the supersonic portion of the flights, since at the subsonic speeds the combined effects of increasing Mach number and decreasing ambient air temperature produced only small changes in the skin temperatures.

Figure 4 shows the nose of the X-1B, where both skin-temperature and pressure measurements were made at intervals along the nose between station 0 and station 55.0. The pressure data are plotted as pressure coefficients at the bottom of the figure. The measured skin temperatures are shown in the upper part of the figure as the open symbols. The skin temperature decreases over the forward part of the nose cone, the laminar flow calculations showing fairly good agreement. This variation is followed by a region of no change in the skin temperature and then an increase toward the rear of the nose cone where the calculated turbulent flat-plate and cone temperatures are approached. In this region the nose-cone

shape asymptotically approaches the cylindrical shape of the fuselage, and the pressure drops to near the free-stream value. The overall temperature variations that are shown suggest that transition from laminar to turbulent flow takes place along the nose at about 25 to 30 percent of the nose-cone length, fully turbulent flow developing at the rear of the nose cone. A summary of various wind-tunnel data on cones and bodies of revolution indicated this general transitional area.

The skin on the nose cone was relatively thin in comparison with that on other areas on the airplane. The effects of varying skin thickness on the skin temperatures can be seen in figure 5. Figure 5 shows the spanwise distributions of maximum temperatures on the upper wing skin at the 66-percent-chord line and at the leading edge. The spanwise variation in the skin thickness is shown below. The temperature variations indicate an inverse relationship between the skin temperature and the skin thickness at both chordwise positions. The trend which would give rise to thermoelastic considerations at higher temperature levels is clearly seen in the data here.

The calculated temperatures, shown by the dashed lines in figure 5, were based on a constant spanwise heating input, laminar for the leading edge and turbulent for the 66-percent-chord line; and the same variations due to thickness are seen in the calculated temperatures.

The data in figure 5 also illustrate the differences in the skin temperature with chordwise position. Both top and bottom skin temperatures were measured at several chordwise positions at about midsemispan and near the tip of the wing. These data are presented in figure 6. In this figure the calculated temperatures were estimated on the basis of zero angle of attack. No detailed consideration is given to the effects of angle of attack on the measured temperatures; however, from an overall standpoint it should be recalled from figure 2 that the angles of attack were positive during the flight and were on the order of 2° to 10°.

The data of figure 6 illustrate several interesting trends. First, notice the chordwise temperature gradients that are shown at the midsemispan station. The higher temperatures are experienced at the leading edge and the trailing edge (which at this location is the outboard tip of the flap), and the lower temperatures are experienced on the thicker skinned wing box section.

Secondly, note the differences in temperature between the top and bottom skins at the two span stations, the bottom skin temperature being higher in both cases. At the tip station, the fairly large differences seen between the top and bottom skin suggest that the flow might be partly separated in this area.

The approximate calculations, which were based on the assumption of laminar flow over the leading-edge section and turbulent flow over the remainder of the chord, give a fairly good overall estimate of the skin temperatures at the midsemispan station. At the tip station the calculations agree fairly well with the bottom skin temperature; however, they indicate an overestimate of the top skin temperature, probably because of the flow effects previously mentioned.

An example of the internal temperatures that were measured through the wing is seen in figure 7. Shown in the figure are the front wing spars at about midsemispan on the X-1B and the X-1E. The temperatures were measured at the locations shown by the black dots on the structures, and the values are given on the right-hand side of the figure. The higher temperatures shown for the X-1B were measured on the skin a slight distance from the spar.

In order to give an indication of the temperature rise that has taken place in the internal structure, it is worthwhile to mention that the ambient air temperatures were between -70° F and -90° F and that the assumed turbulent adiabatic wall temperatures were on the order of 200° F for the highest Mach numbers shown here. The measured internal temperatures are relatively low and show only slight temperature gradients across the thickness of the X-1B wing, the lower temperature being obtained on the spar center line. Essentially no differences are seen on the thick spar construction of the X-1E wing, the heavier type of construction of the X-1E having a temperature-neutralizing tendency due to the higher heat capacity. The thermal lag effect is also seen in figure 6 by the increase in the measured temperatures as the Mach number decreases in the later portions of the flights.

Effects of material thickness differences are also seen in the measured leading-edge temperatures. These data are shown in figure 8 in time-history form together with time histories of the assumed laminar adiabatic wall temperatures. The locations at which the temperatures were measured are shown by the dark points on the leading-edge sketches, and the material thicknesses are given at these locations. Values of the average heat-transfer coefficients utilized for the calculated temperatures are shown below the sketches. The calculated temperatures are seen to agree very well with the measured data.

Maximum temperatures on the same order of magnitude were measured on the wing and vertical-tail leading edges of the X-1B. For comparison, the temperatures that were measured at the rear of the solid leading edge of the X-1E are seen in the middle of the figure. It will be noticed that the maximum measured temperature was on the order of 20° F. The high heat capacity of the solid leading edge is the contributing factor to the small rise in the temperature measured at this location. The calculated skin temperature is shown to agree very well with the

measured data; however, this result is not considered significant because the measured temperatures are relatively low. (For example, a 50-percent reduction in the assumed heat-transfer coefficient at this point would produce a decrease in the calculated maximum temperature of 7° F.)

The chordwise variation in the vertical-tail temperatures is shown in figure 9 for a time near maximum Mach number at near midspan. The temperatures were measured on the skin and spar center lines at the locations shown by the black dots on the sketch. No appreciable gradients are seen in the chordwise variation of the measured skin temperature.

Transition from laminar to turbulent flow was assumed to take place at the point where the leading-edge section attaches to the front spar because inspection revealed a relatively large discontinuity in the skin at this point. Skin temperatures calculated from the average heat-transfer coefficients shown and based on these assumptions agree fairly well with the measured trends in the leading-edge region but deviate somewhat over the remainder of the chord and give a conservative overall estimate in this region.

CONCLUDING REMARKS

Skin and structural temperatures have been obtained on the X-1B and X-1E research airplanes under transient aerodynamic heating conditions at speeds up to Mach numbers near 2.0. Extensive temperature measurements were obtained throughout the X-1B airplane, and temperature distributions are shown on the nose cone, the wing, and the vertical tail. Temperatures for the X-1E wing leading edge and internal wing structure were compared with similar data for the X-1B.

No critical skin and structural temperatures were obtained on the two airplanes over the range of these tests.

Simplified calculations of the skin temperatures in the laminar-flow regions of the nose cone and the leading edges agreed favorably with the general trends in the measured data. The flat-plate skin-temperature calculations in the turbulent-flow regions agreed favorably with the measured data on the nose cone and at the midsemispan station of the wing but overestimated the vertical-tail skin temperatures and also the upper wing skin temperature near the wing tip. The relatively low values of the upper skin temperatures that were measured at the wing tip were believed to be caused by separated-flow effects in this region.

High-Speed Flight Station,
National Advisory Committee for Aeronautics,
Edwards, Calif., March 6, 1957.

REFERENCE

1. Stine, Howard A., and Wanlass, Kent: Theoretical and Experimental Investigation of Aerodynamic-Heating and Isothermal Heat-Transfer Parameters on a Hemispherical Nose With Laminar Boundary Layer at Supersonic Mach Numbers. NACA TN 3344, 1954.

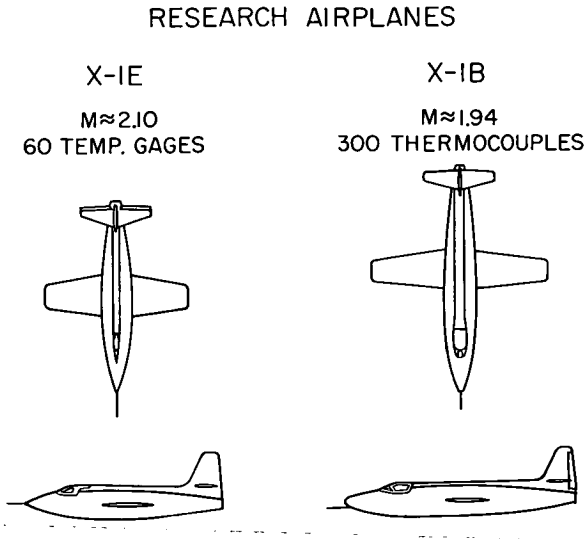

Figure 1

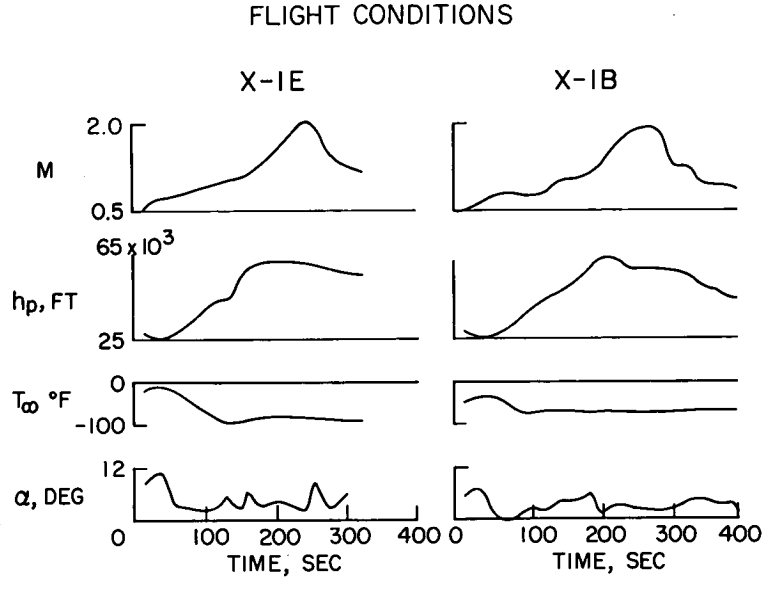

Figure 2

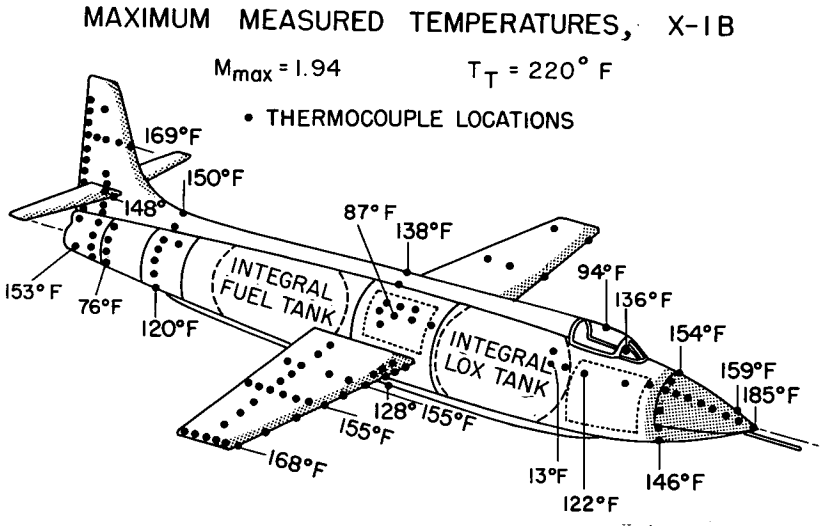

Figure 3

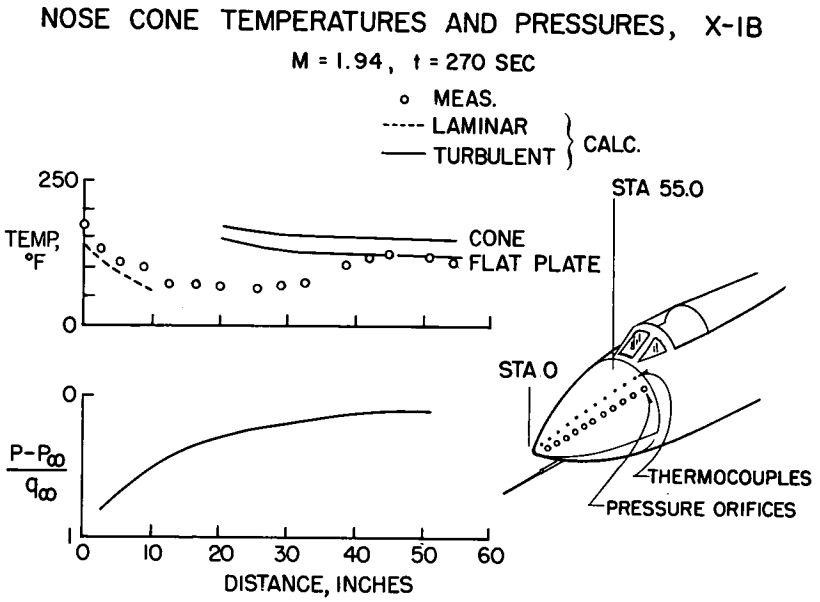

Figure 4

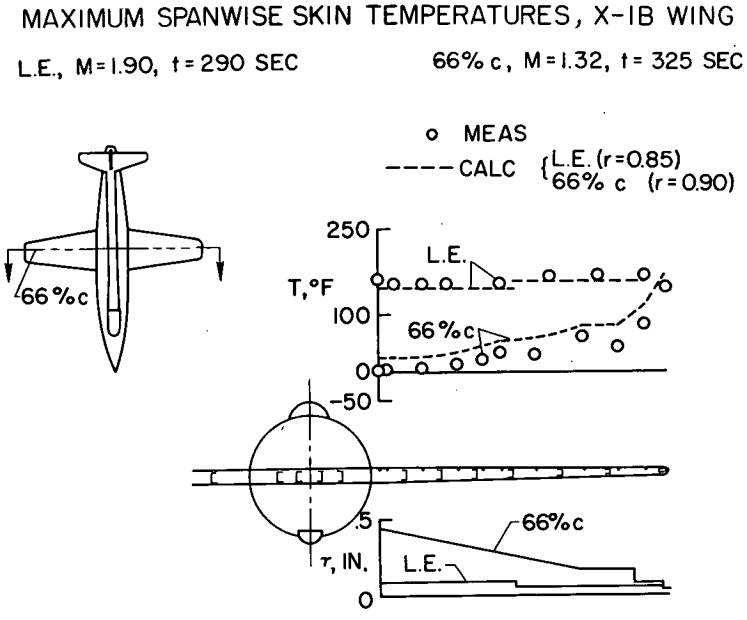

Figure 5

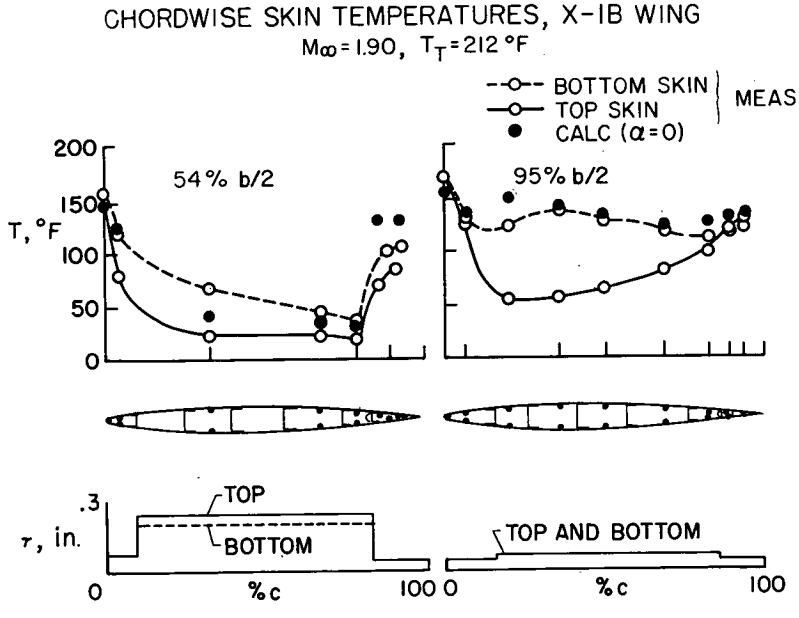

Figure 6

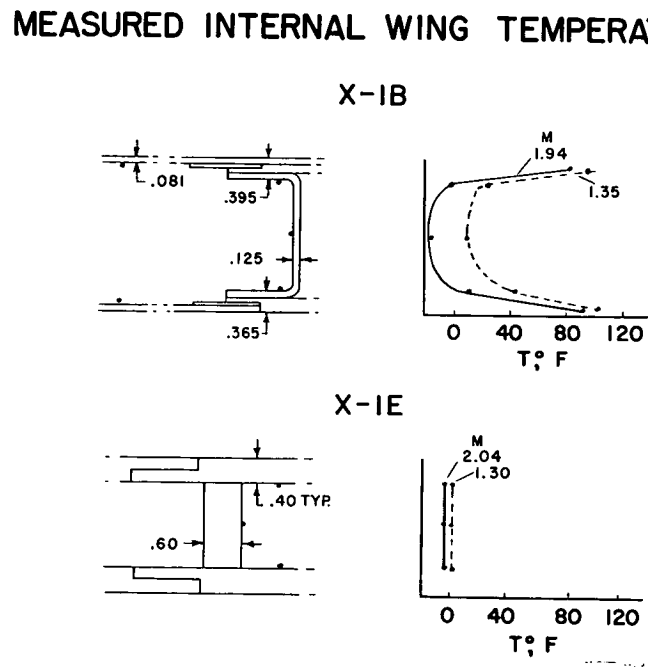

Figure 7

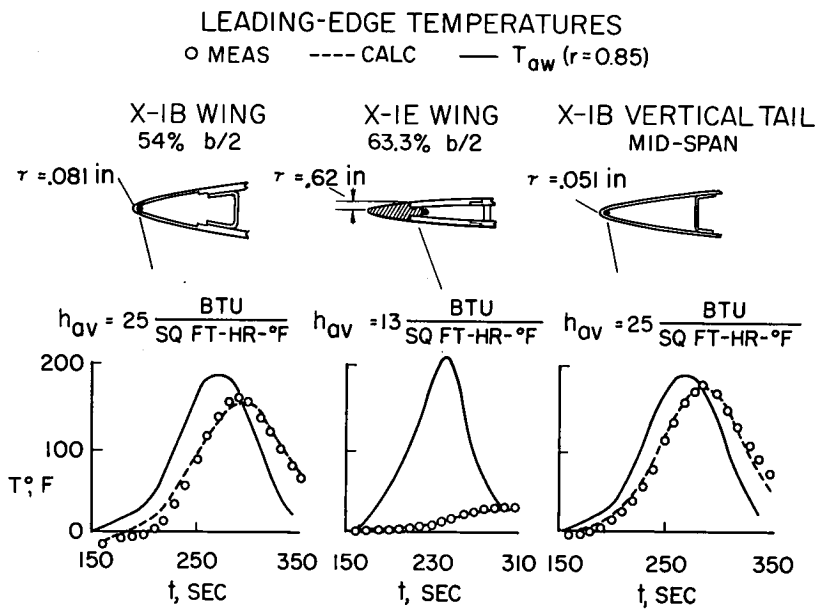

Figure 8

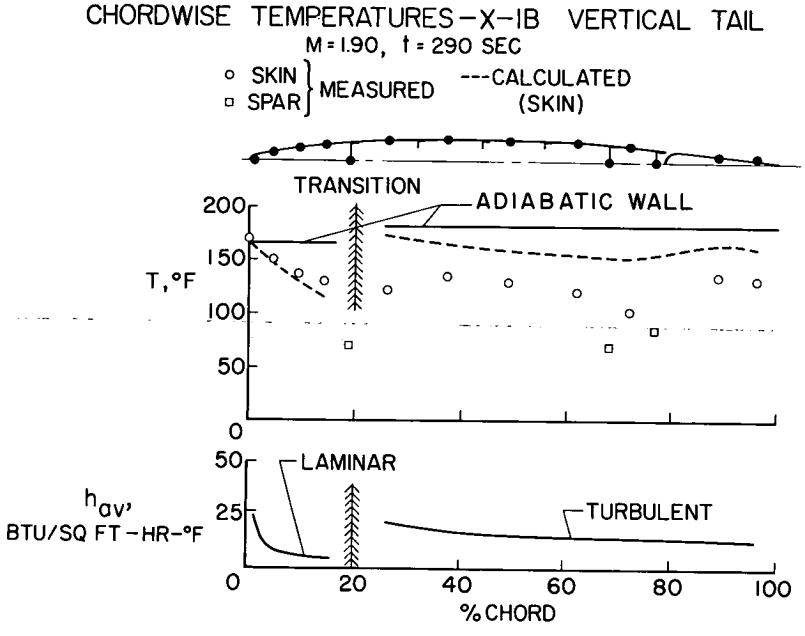
CHORDWISE TEMPERATURES – X-1B VERTICAL TAIL
M = 1.90, t = 290 SEC
SKIN
SPAR
MEASURED
---CALCULATED (SKIN)
TRANSITION
ADIABATIC WALL
T, °F
200
150
100
50
0
LAMINAR
TURBULENT
h_{av}, BTU/SQ FT-HR-°F
50
25
0
20
40
60
80
100
% CHORD

Figure 9